Rose-Hulman Institute of Technology

2008 ASME West Coast HPV Competition

Single Rider Entry Team 35

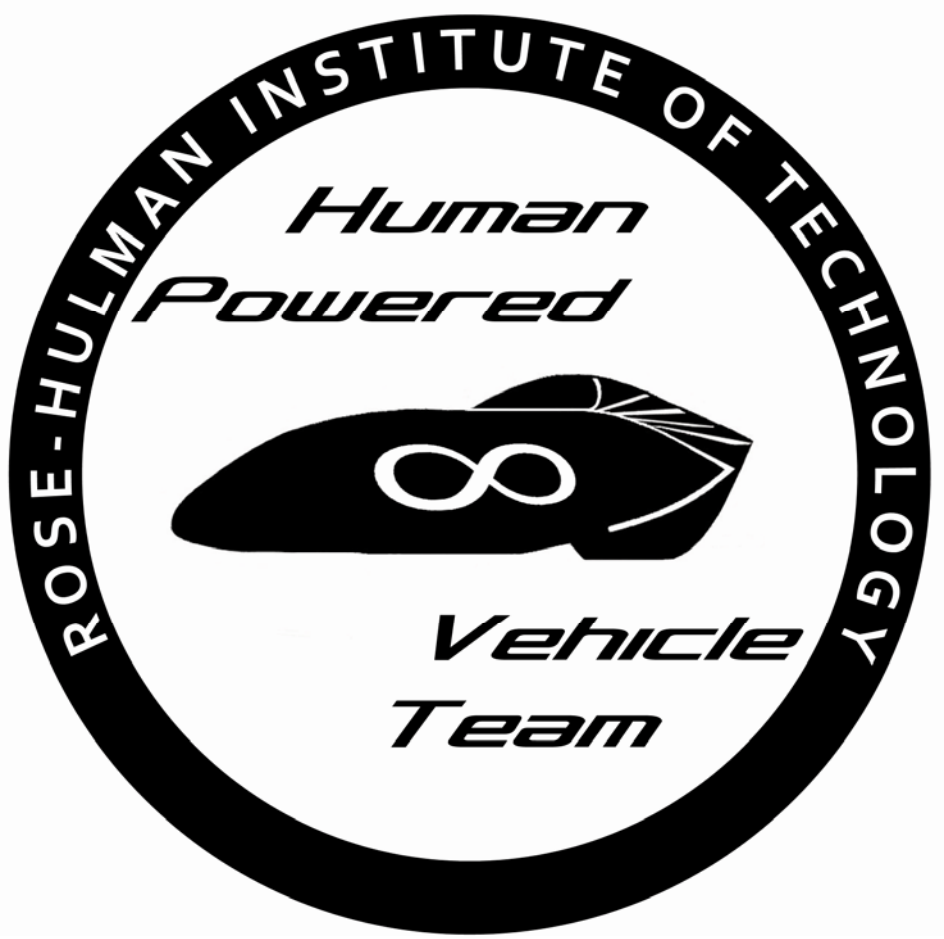

Team Members

Tommy Roberts
Zach Goff
Danny Sing
Molly Nelis
Chris Wlezien
Ariel Young
Jeffery Van Treuren
Blake Lin

Rachelle Cobb
Nathan Wendt
Ed Mayhew
Andy Boneff
Justin Gerretse
Rebekah Forsyth
Nobutoshi Hiro
Cory Pate

Contents

Contents I
Abstract II
1 Design and Innovation 1
1.1 Goals 1
1.2 Quality Function Deployment 1
1.3 Research 3
1.4 Math Modeling 3
1.5 Fairing Selection 6
1.6 Internally Steered Hub 8
1.7 Field of View and Visibility 9
2 Analysis 9
2.1 Aerodynamic Analysis 9
2.2 Stability Analysis 11
2.3 Internally Steered Hub Analysis 11
2.4 Roll Cage Strength 12
3 Testing 13
3.1 Stability Testing 13
3.2 Abrasion Resistance 17
3.3 3 Point Bend Test 18
3.4 Roll Cage Testing 20
4 Safety 21
Appendix 1 Abrasion Resistance Data 22
Appendix 2 Costs 23
References 25

Abstract

Over the past three years, the Rose-Hulman HPV team has refined the short wheel base, lowracer recumbent to be strong competitor at the human powered vehicle competition. In 2007, the R5 placed 2nd at the East Coast HPV challenge. For 2008, the Rose-Hulman Infinity will be smaller, safer and more stable than its previous entries. Figure 1 details the evolution of the Rose-Hulman design over the past three years.

Figure 1 - Evolution of Design
(Left) 2006 Hazard (Middle) 2007 R5 (Right) 2008 Infinity

The Infinity is the next step in the evolution of our lowracer design. From our experiences with the R5, we knew that the lowracer design is inherently fast and maneuverable. This year, we have set out to prove that it can also be stable and safe. The clear canopy of the R5 is replaced with a traditional windshield in front of the riders head. The steeper angle of the windshield increases the forward visibility for the rider, while the new more upright seating position allows the rider to gain tighter control of the vehicle.

The Infinity will also be an evolution from previous designs in that it is the first Rose-Hulman entry to be an entirely monocoque design. Using carbon fiber, Kevlar, and Nomex honeycomb, this vehicle will use the fairing as its frame and roll cage. By changing the fairing into a structural member, the overall safety of the vehicle will increase dramatically, simultaneously freeing up interior space and acting as an exoskeleton.

Rose-Hulman's previous entries, The Hautian Hazard and R5 had top speeds of 38 and 36 mph. With the Infinity, our team goal is an increase our ASME HPVC sprint speed to 40 mph with a dramatic increase in handling and maneuverability. We believe through extensive research, analysis, and real-world testing, our vehicle has the capability of being even more competitive than our previous entries, while simultaneously being among the safest vehicles in field.

1 Design and Innovation

The design of the vehicle began by defining vehicle goals. A quality function deployment was completed to identify the most important design features of the vehicle.

1.1 Goals

In September, our team created a list of strengths and weaknesses for the 2007 R5. This list of brainstorming ideas helped us determine what the goals for the 2008 project would be. Table 1 shows the topics discussed and improvements decided upon.

Table 1 - Brainstorming Improvements on 2007 Vehicle

Strengths	Weaknesses	Improvements
Solid fairing	Weight	Lighter bike
Crashworthiness	Gearing/shifting	Visibility
Landing gear	Time to change wheels	Stability
Fairing height	Tiller steering	Simpler drive train
Narrow Q factor	Surface finish	
Protected derailleur	Visibility	
	Overall length	
	Complex drive train	
	Laminar flow design	

From this brainstorming session, we were able to hone in on the most obvious areas of improvement over the year before. Visibility, stability, and weight most often came up as areas needed for improvement from the year before.

1.2 Quality Function Deployment

Once we brainstormed our own list of improvements needed from the year before, our team employed a Quality Function Deployment (QFD) tool in order to identify the most important issues associated with the human powered vehicle design. Figure 2 details the QFD done for a human powered vehicle at the ASME HPVC.

The QFD let our team look at the customer and design requirements in order to determine the relative importance of each aspect of a human powered vehicle design. The highlighted red row of the QFD shows the relative importance of each of our defined design requirements. From this line, you can see that the most important aspects of the design are vehicle height, weight, number of wheels, seatback angle, and field of view. The result of this exercise was an increased understanding on the value associated with each of the design characteristics.

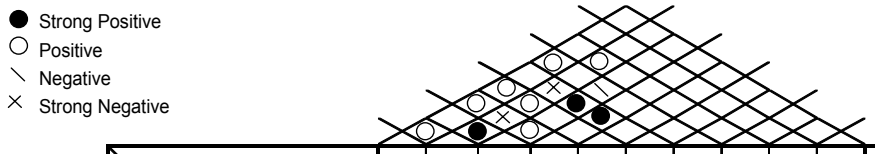

Customer Requirements (WHATs) \ Design Requirements (HOWs)	Vehicle Height	Weight	# Wheels	Cost	Max Rider Height	Development Time	Seatback Angle	Crank Length	Field of View	Turn Radius	**Customer Importance**	Current Competition	Planned Vehicle	Improvement Ratio	Sales Points	Absolute Improvement	Relative Improvement
Fast	9	9	9	1	9	3	9	9	1	1	5	4	5	1.3	2	13	0.2
Stable	9		3			1	9	1	9	9	5	5	5	1.0	2	10	0.2
Safe		1	1	3		3			9	1	5	4	5	1.3	2	13	0.2
Durable		1		1		1					3	2	4	2.0	1	6	0.1
Time to Deliver		1	1	1		9					3	4	3	0.8	1	2.3	0.0
Lightweight Vehicle	1	9	3	9	1	3					4	5	4	0.8	2	6.4	0.1
Repairable		3		1		1			3		2	3	3	1.0	1	2	0.0
Low Cost		9	3	9	1	3					1	3	3	1.0	1	1	0.0
Innovative		3		1		3					3	3	4	1.3	1	4	0.1
Maneuverable	1	1	1				3		9	3	3	5	5	1.0	1	3	0.1
Abs. Importance	3.74	3.90	3.22	2.31	2.12	2.60	3.73	2.16	4.38	2.19	30						1
Rel. Importance	0.12	0.13	0.11	0.08	0.07	0.09	0.12	0.07	0.14	0.07	1						
Current Competition	10	36	2	?	6	2				40							
Improvement Direction	▲	▲	▲	○	▲	○				▲							
target value	15	200	0.75	20	4	2				75							
units	in	lb	unit	$	ft	ppl	deg	mm	deg	ft							

Figure 2 - House of Quality

The QFD gave us an idea for how to progress in the design of the vehicle. Below is a list of goals and constraints for the 2008 vehicle. We removed number of wheels from important considerations because we have thoroughly discussed the merits of three and two wheeled designs in our 2006 and 2007 design reports. The vehicle is an evolution of the previous design, and as such will be two wheels. This will also allow us to focus on new areas of research for this design report, instead of re-hashing old material.

Table 2 - Team Goals and Constraints

Team Goal	• 40 mph HPVC Sprint Speed • Increase field of view • Improve seat angle • Decrease weight • Improvements on stability and • Improvements on maneuverability

Constraints	• 25 ft. turn radius • Brake from 15 to 0 mph in ≤ 20 *ft*. • Additional redundant braking system • Travel 100 ft. in straight line • Equivalent to chrome-molly steel tube roll cage of 1.5" OD and wall thickness of .049 • Safety harness (seatbelt) ≥ 3 points • Rider protection from sliding

1.3 Research

In 2007, the Rose-Hulman HPV team went to the Nissan One Hour Record event. Here, we had a chance to view a number of different record-setting designs. Through our experiences, we learned a great deal about the fastest HPVs in the world, and wanted to take some of their construction methods with us into the 2008 vehicle. This prompted us to look at the fastest bikes around the world and research on their construction. Table 3 details the results of our research. What we learned from this research is that monocoque vehicles have the best potential to achieve low weights. While some monocoque vehicles weigh as much as frame/fairing vehicles, even the heaviest vehicles are less than the 75 pounds the 2007 R5 was. As a result of this research, we set a goal for ourselves to achieve a 50 pound weight vehicle.

Table 3 - Prior Art of HPVs

Bike	Length	Width	Weight	Construction
Varna Diablo 2	8 ft	16 in	60 lbs	Monocoque, foam core
Barracuda	9.5 ft	18.5 in	60 lbs	steel frame, fiberglass fairing
Kingcycle Mango	6.33 ft	15.7 in	36 lbs	Monocoque, honeycomb core
Blue Yonder	10.8 ft	22.8 in	26.5 lbs	Monocoque
Varna Clone	8 ft	16 in	40 lbs	Monocoque, honeycomb core
Evie II	8.85 ft	14.4 in	53 lbs	Ti frame, Carbon/Kevlar body
Moby	10.9 ft	19 in	74 lbs	steel frame, fiberglass fairing

1.4 Math Modeling

In order to develop criteria and set goals for our rolling and air resistance values, we created a Simulink program to graph the velocity of an HPV in a sprint. In order to make use of this program, a theoretical human power output was needed. The figure below represents data taken by NASA to gauge human performance.

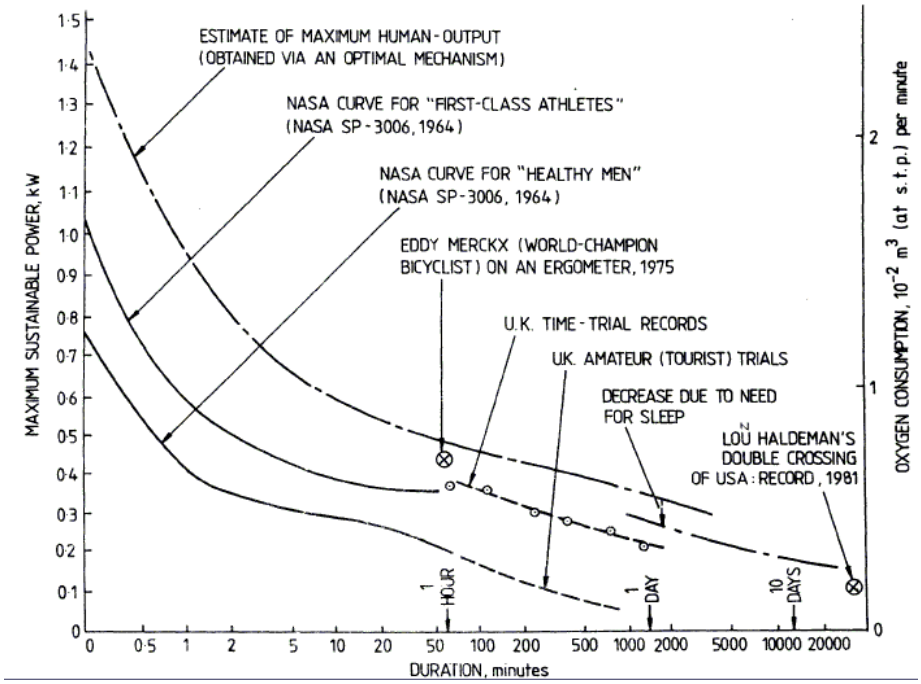

Figure 3 - Power Estimate Curves for Human Output

Using figure 3 as a reference, the theoretical maximum output for a healthy male over one minute is 400 watts. This value is what we used in our simulations For the coefficient of rolling resistance, we used a value of .003. This value is a conservative estimate for our Michelin Ecorun tires. Full rolling resistance tests to support this value were shown during our 2007 design report. Since these tests have been run previously by our team, we see no reason to further elaborate on the subject.

This left our team with two main variables, weight and coefficient of drag times area (CdA). From our research into current HPVs, we determined an estimate for our monocoque design to be 50 pounds. From here, we ran the simulation at numerous CdA values to determine a goal for this parameter.

Using our Simulink program, we created figure 4 and figure 5. These figures show how the bike would accelerate under a constant power output by the rider. Figure 4 shows that using a CdA of .4, our vehicle would hit an estimated 38 mph in the sprint if the run-up is 500 meters long. 38 mph is below our target speed of 40 mph, however lowering the CdA any further could be an unrealistic goal. We hope to use these target numbers as minimums, so any improvements over these goals would help us to the 40 mph sprint speed. Figure 5 shows that using these numbers, our theoretical max speed would around 54 mph. Thus, if the run-up is lengthened to the maximum specified in the rules (600 m) it is very realistic that we could break or exceed our 40 mph goal.

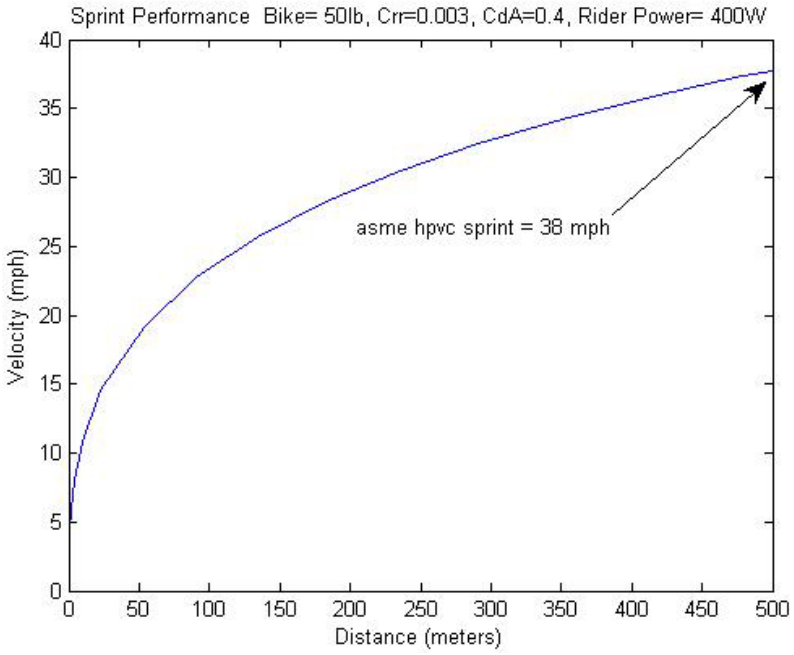

Figure 4 - Sprint Performance of Ideal HPV Entry

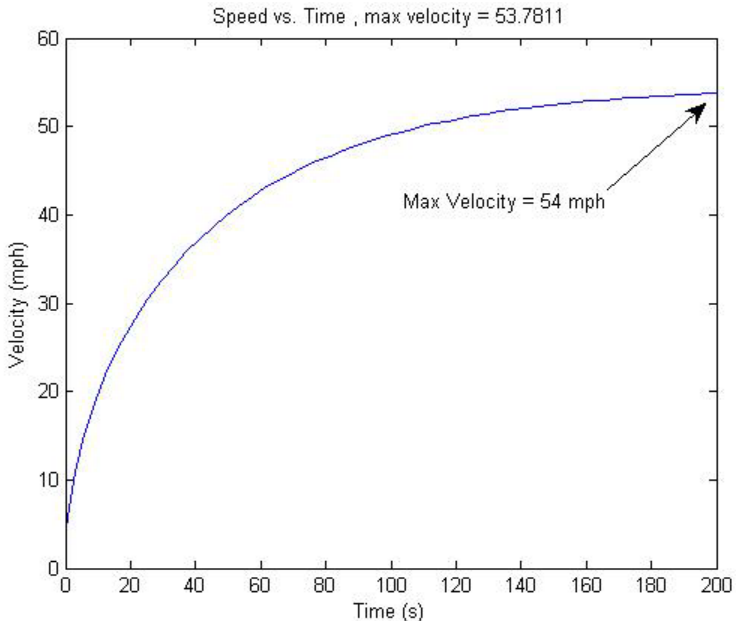

Figure 5 - Max Velocity of Ideal HPV Entry

Using the results from our Simulink program, a summary of design goals for our 2008 entry are tabulated below.

Table 4

Team Goal	40 mph ASME HPVC sprint speed
Aerodynamic Goal	$C_d \cdot A \leq .4\, ft^2$
Rolling Resistance	Tires with $C_{rr} = .003$
Weight	$Weight \leq 50 lbs$
Safety	• 25 ft. turn radius • Brake from 15 to 0 mph in $\leq 20\, ft$. • Additional redundant braking system • Travel 100 ft. in straight line • Equivalent to chrome-molly steel tube roll cage of 1.5" OD and wall thickness of .049 • Safety harness (seatbelt) ≥ 3 points • Rider protection from sliding

At this point, the rider layout, handling, and stability were increasingly important. In order to find our rider geometry, we turned to testing of variable geometry prototype bike which we designed and manufactured. For more information on this test please see the testing section of this report.

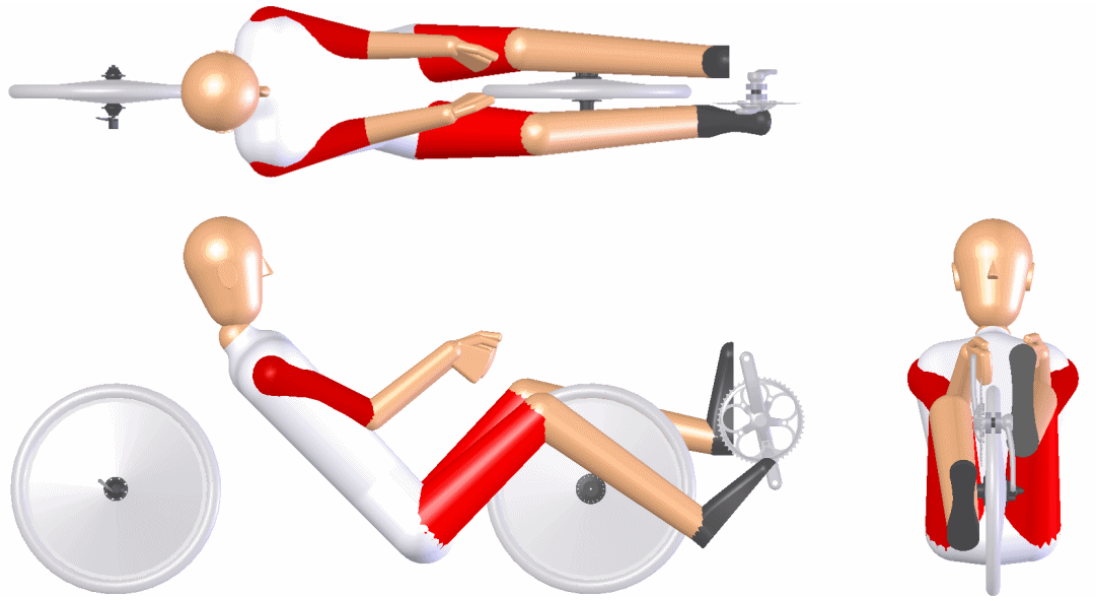

Figure 6 - Rider Layout for Infinity

1.5 Fairing Selection

Once a rider position, wheel base, and crank location were determined, the aerodynamic analysis team created numerous models of possible fairing/vehicle designs using SolidWorks. The three final fairing designs are detailed in figure 7, figure 8 and figure 9.

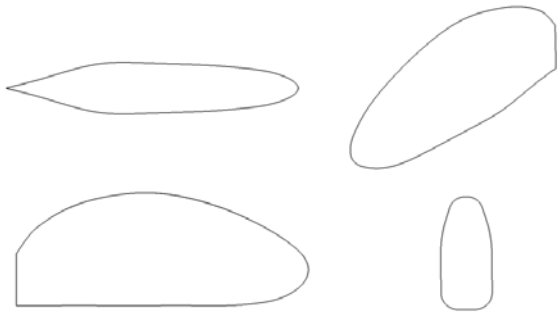

Figure 7 - Egg Fairing

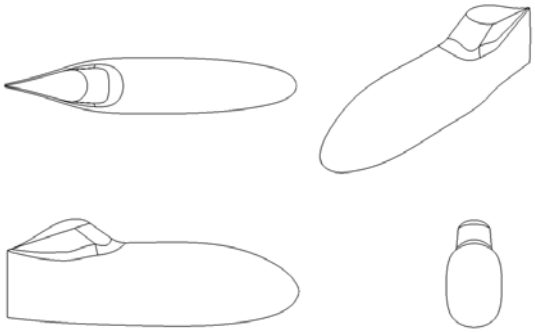

Figure 8 - Infinity Fairing

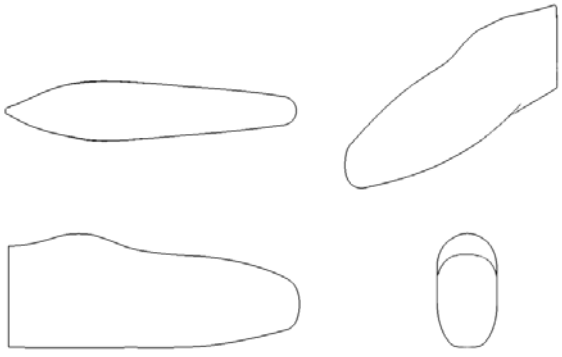

Figure 9 - Black Mamba Fairing

Table 5 - Decision Matrix for Fairing Designs

Design Considered	CdA	Windshield Clarity	Length	Field of View	Least Complex	Weighted Score
	30%	30%	10%	20%	10%	
Final Egg	10	5	5	10	9	7.9
Infinity	9	9	8	8	6	8.4
Black Mamba	5	9	10	8	6	7.4

The decision matrix in table 5 details how we choose the final fairing for our vehicle. To analyze how aerodynamically efficient each design would be we tested each model using COSMOS FloWorks to find the drag forces. More detail on testing the models in FloWorks can be found in the testing section of this report. With the numbers from FloWorks, we were able to assign values to how aerodynamically efficient each design was. After this, windshield clarity was looked at. We decided that head bubble designs would be weighted favorably compared to a design with the windshield integrated into the shape of the bike. Our reasoning for this is that last year we learned how difficult it is for a rider to see clearly through a windshield that has a very gradual and curving slope. Length of the vehicle was also a factor as a small vehicle will be easier to maneuver though a twisted endurance event. Next, a score for field of view was determined. The Egg fairing clearly would have the most field of view, since it would have a large, drape formed windshield over the top. This was rated favorably compared to head bubble design which would primarily have a windshield in front of the riders face. Finally, complexity was an issue taken into account. It is very easy to sand and shape a mold for one continuous curve. Head bubble style designs with more curves will take longer to sculpt. Once all these values were weighted, it was determined that the Infinity fairing was the best design.

1.6 Internally Steered Hub

The purpose of the hub steer design on the 2008 Infinity is to reduce the overall height of the bike and to increase the ease of steering from the 2007 R5 with its unstable tiller steer design. The hub steer is built with no fork; rather, it has a push/pull cable linking the handle bars and U-joint that allows our rider to control its rotation about the kingpin. It has bearings off to the side of the pin which a shell/housing, U-joint, and ultimately the wheel, brake disk, and cassette are attached to. This whole shell/housing assembly revolves around the kingpin and U-joint and this allows us to mount the wheel to the bike from the side instead of using a conventional fork and headtube. We have fabricated three iterations in order to develop the concept. Our first iteration had no drive, but had an adjustable rake feature that allowed us to perform our optimization testing when it was mounted to the variable geometry bike. Our second was driven and built onto our prototype bike. Our third iteration includes disk brake mounts and a 9 speed cassette to allow front wheel drive.

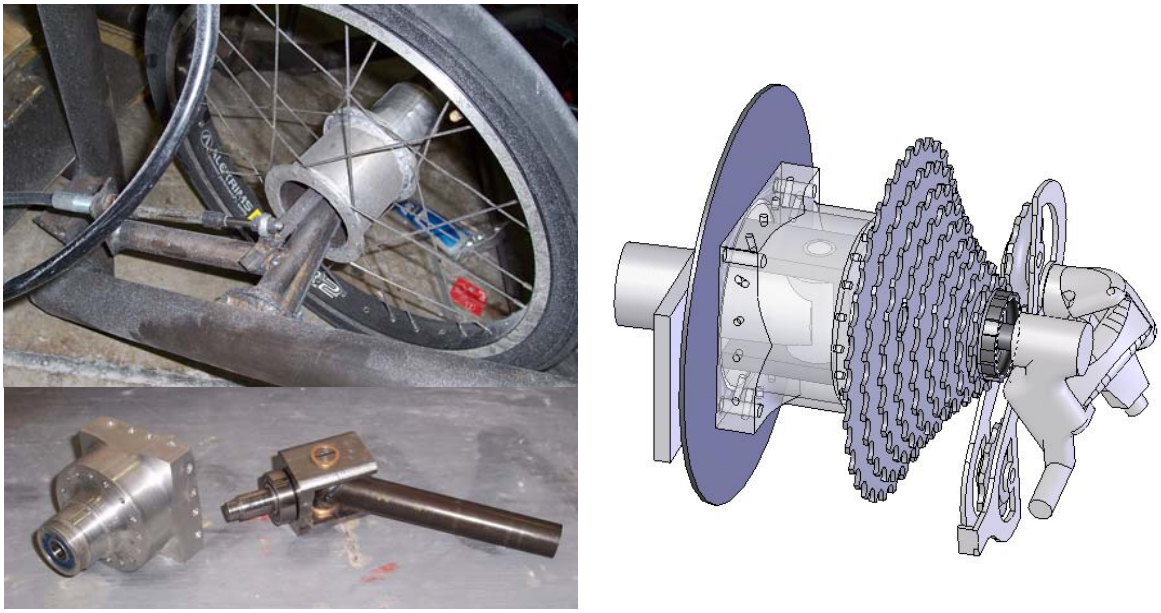

Figure 10 - Hub Steer Iterations (Top Left) 1st Iteration on variable geometry bike (Bottom Left) 2nd Iteration off of prototype bike (Right) 3rd iteration

1.7 Field of View and Visibility

Figure 11 – (Left) The Infinity will have a flat sheet of plastic in a 2-d bend (Right) Long gradual canopies have great side visibility, but are hard to see forward through such a shallow angle.

From our experiences last year, we understood that windshields with very gradual and curving slopes are more difficult to see through. The intention this year was to ensure that visibility would not be an issue. By using a thin flat sheet of plastic at a nearly vertical angle, our vision will be clear and the rider will be more stable during the sprint event.

2 Analysis

2.1 Aerodynamic Analysis

Using FloWorks, each of our possible fairing designs was sent through a computational fluid dynamic simulation. The results were then scrutinized and used to continually

develop further better fairing models. In the end, three possible designs were chosen as finalists.

Figure 12 below details the pressure gradients and velocity flow lines for each of the final three vehicle models. Each of the models was run under the same conditions. The computational domain was set so that ground effect would be accounted for. Also, all the models were run under turbulent flow conditions. Floworks was able to calculate force exerted on the body, and using the aerodynamic force equation 1, we converted these numbers into CdA vales. Table 6 shows the results of running each of our finalist fairing designs through FloWorks. The CdA values for each were used to determine the values for the fairing decision matrix in table 5.

Equation 1 $$Force = \frac{1}{2}\rho C_d A V^2$$

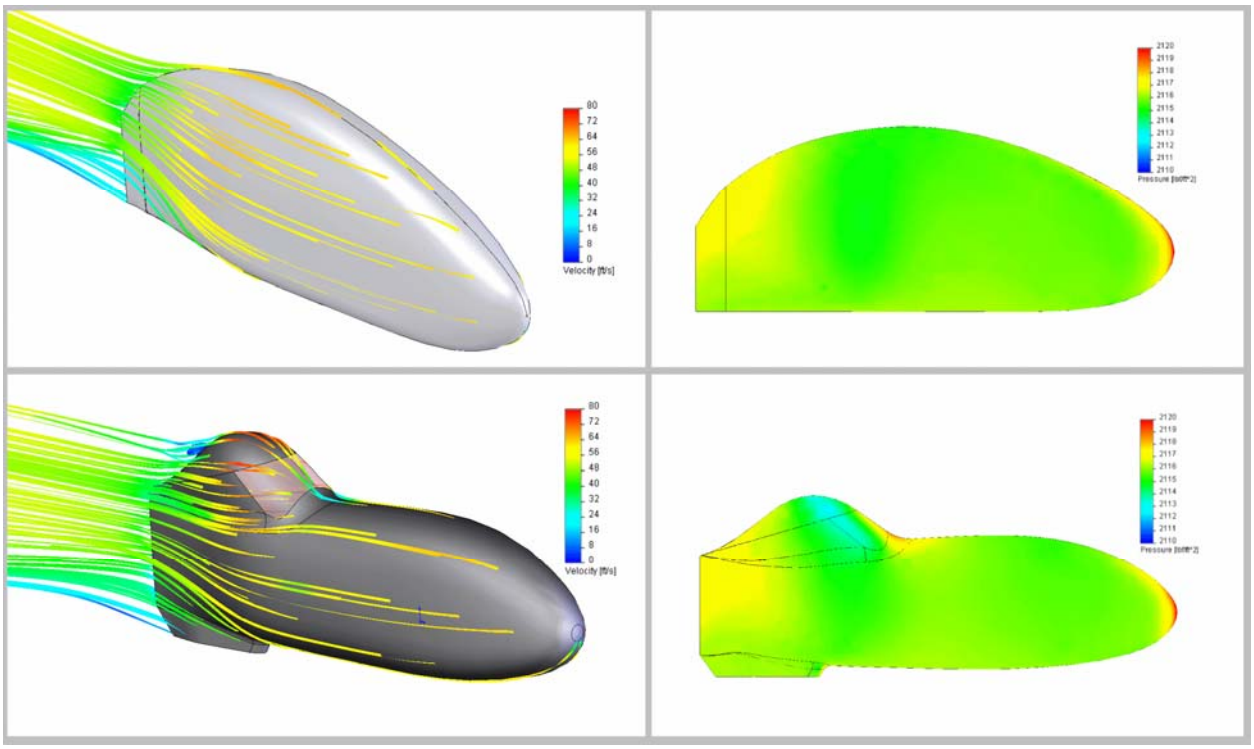

Figure 12 - Floworks Examples of Giant Egg and Infinity fairings

Table 6 - Summary of CFD testing on Fairing Designs

Fairing Design	CdA Value	Speed (m/.s)	Force (Newtons)	Mesh Refinement (Accuracy)
Final Egg	0.29	18.29	5.33	5
Infinity	0.318	18.29	5.78	5
Black Mamba	0.47	18.29	8.55	5
Final Egg	0.297	18.29	5.40	7
Infinity	0.313	18.29	5.69	7
Black Mamba	0.43	18.29	7.89	7

2.2 Stability Analysis

To design a vehicle that handles properly, equation 2 predicts the stability of a certain bicycle geometry [7]. A K5 value of 0.5 represents the handling of a typical lowracer, while a value of 1.2 is appropriate for an inexperienced rider. Ultra low K5 values below 0.5 result in fast steering response and thus more difficult control of the vehicle. Trail, T is limited to a maximum of 5" or else excessive fork flop will make low speed handling very difficult. M is total mass of the vehicle, Kx the radius of gyration which corresponds to seatback angle, h is the distance from the center of gravity to ground and B is the horizontal distance from the center of gravity to the rear wheel contact point. The center of gravity location can also be approximated at the rider's belly button.

Equation 2

$$T = K5 \cdot \frac{B}{M}\left(\frac{1}{Kx^2} + \frac{1}{h^2}\right)$$

By measuring the vehicle geometry, the handling characteristic K5 can be determined. To prove that this relationship is indeed valid, a variable geometry test vehicle is built and presented in the testing section. Results from this stability analysis are presented and compared with test results.

2.3 Internally Steered Hub Analysis

The design constraint of the internally steered hub was foremost geometric. If the hub could not fit within the allotted space, it was not practical to use. Once a properly sized hub was designed, it is necessary to select an appropriate material to assure its structural integrity. Two problem areas are identified. The axle diameter reduction between the two support bearings and the bearing loads.

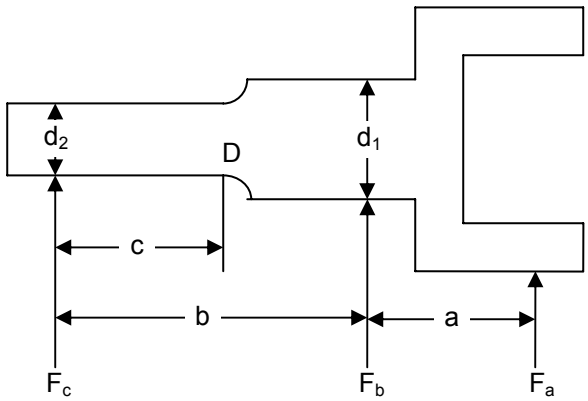

Figure 13: Internally Steered Hub Analysis Dimensions

By applying fundamental concepts from statics and materials, a system of equations can be developed and solved for the maximum stress at D and the bearing forces F_c and F_b.

The appropriate stress concentration factor, K for the geometry of the axle at point D is 1.3 [5].

Equation 3
$$\sigma = \frac{32KaF_a cd_2^{\ 3}}{\pi b}$$

Equation 4
$$F_b = -\frac{F_a(a+b)}{b}$$

Equation 5
$$F_c = -\frac{aF_a}{b}$$

Evaluating the previous equations with the known geometry of the hub as well as assuming a 210lb vehicle with 60% weight carried on the front hub, the maximum tensile stress is 21000 psi and the bearing forces are 63 lbf and 188 lbf for the outer and inner bearings. The bearing forces are well within the specified load ratings of the chosen bearings. To allow a factor of safety of at least 3, a metal with a yield stress of 63,000 psi should be chosen. The chrome-molly family of materials such as 4130 or 4340 in the annealed state meets this yield strength requirement and will be used.

2.4 Roll Cage Strength

A mock up of the roll cage that is in our bike was constructed using layers of (starting on the inside) 1 layer of Kevlar, 3 layers of carbon fiber, Nomex honeycomb core, 3 layers of carbon fiber, and a layer of Kevlar and carbon fiber bi-weave. The layers were vacuum formed to the mold and allowed to dry. Once the roll cage was completed, it was placed in a tensile test machine in the vertical orientation. A load of 507 lbf was applied to the roll cage. Next the roll cage was loaded in the side load orientation. A load of greater than 269 lbf was applied. In both load cases, the roll cage demonstrated that it met the requirements for load carrying and for deformation.

After it was established that the roll cage met the specifications from the rule book, it was decided to reload the roll cage in the vertical orientation and a force of 765 lbf was applied before there was significant deformation. The Nomex honeycomb demonstrated a remarkable resilience in that after it was deformed, it recovered to its original shape and material properties. Subsequent testing also showed the durability of the roll cage after various alternate loadings.

In order estimate the maximum stresses that would be carried by the roll cage in each of the loading configurations, calculations were performed using a model of the bike as a combination simply supported and cantilevered beams. In the top load case, a maximum bending stress of 13 ksi was found in the middle of the top member. In the side walls, the compressive stress was about 500 psi.

Equation 6
$$I = \frac{bT^3}{12} - \frac{b(T-0.21)^3}{12}$$

Equation 7
$$\sigma_{\max,bend} = \frac{FLT}{8I}$$

Equation 8
$$\sigma_{\max,comp} = \frac{F}{2b(T-0.21)}$$

In the side load case, the roll cage was modeled as shown with the bottom member fixed where the wheel mount would be and the load being applied approximately where the shoulder of the bike would contact the ground. The maximum bending stress in this model was calculated to be 30 ksi. The equations used were similar to the equations used for the top load case. The ultimate tensile strength of the carbon fiber weave that is used in our bike is approximately 600 ksi which is much greater than the values calculated.

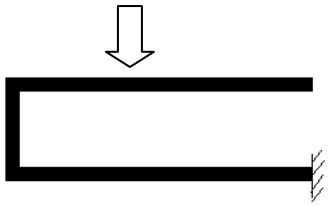

Figure 14 - Roll Hoop Approximation

3 Testing

A significant amount of testing was used to design, fabricate and validate the vehicle. Two specific tests were used to develop the vehicle, and two tests are planned once vehicle fabrication is completed. In order to further understand and optimize the ride-ability of the new vehicle, an adjustable bike frame was developed to test the effects of varying headtube angles, seatback angles, and wheelbase length. To evaluate the strength of a monocoque frame and fairing, several composite sandwiches were assessed under a 3 point bend test. These tests are presented in the following subsections. Future testing of the vehicle will be done after fabrication to validate the design and optimize its performance. These tests will be discussed at the design presentation.

3.1 Stability Testing

One of the design factors that plagued last year's entry was the rideability of the vehicle. Poor stability at moderate speeds made it impractical to use the full aerodynamic fairing on a road course resulting in severe aerodynamic penalties. In order to optimize ride-ability of this year's vehicle, an adjustable bike frame was built which allowed a design of experiments to be performed on changes to headtube angle, seatback angle and wheelbase length. One way to quantify rideability is the riders input to the handlebars, specifically handlebar deflection. By testing along a strait path, handlebar deflection can

be seen as deviation from ideal strait line motion. Therefore, the bike geometry that yields the least handlebar deflection in straight-line motion is the most rideable.

To perform a measurement, the test bike was brought up to a speed of 25 mph and data capture occurred for 25 seconds. Steering deflection was found to be highly dependent on vehicle speed and so this relatively short time period prevented variances in deceleration from drastically affecting results. To capture data from a test run, a potentiometer was attached to the handlebars and the voltage output was captured with Vernier's LabPro data capture system. Because the bike had to be launched by a tow vehicle due to lack of a drive train, the first 10 seconds of data are ignored to allow for any rider corrections after the tow vehicle and test bike were separated.

In order to minimize the time necessary to complete the testing, an L_9 Taguchi matrix is used. The three control factors are headtube angle, seatback angle, and wheelbase length. Each control factor has three levels: low medium and high. Physical values can be seen in table 7. The noise factors are mainly a result of human error in riding the test bike and vary based on experience. By maintaining the same rider throughout all trials, experience can be judged as low for the first set of measurements, medium for the next set and lastly high.

Table 7 - Control Factors

	Headtube Angle (deg)	Seatback Angle (deg)	Wheelbase (in)
Low-1	15	40	48
Medium-2	20	50	54
High-3	35	65	59

Randomizing the order of trials prevents biasing from affecting the results. Once all trials are run, the total angular deflection for a trial is used as the signal for the Taguchi matrix. A completed matrix is shown in table 8.

Table 8 - Stability Matrix

Trial #	Headtube Angle	Seatback Angle	Wheel Base	Inexperienced Rider	Intermediate Rider	Experienced Rider
1	1	1	1	3.87	6.8	4.32
2	1	2	2	4.66	5.22	4.27
3	1	3	3	4.89	5.62	5
4	2	1	2	4.66	3.48	5.16
5	2	2	3	5.3	5.58	3.84
6	2	3	1	4.75	2.94	5.2
7	3	1	3	3.98	5.94	4.07
8	3	2	1	3.72	4.33	4.23
9	3	3	2	3.67	3.48	4.14

Using Minitab to analyze the data, the signal to noise ratios for a smaller-is-better cost function can be seen in figure 15. Choosing the highest S/N ratio for each control factor will yield an optimal rideability of the vehicle. Therefore, the best design is a high headtube angle, high seatback angle, and medium wheelbase. Note that these results agree with the stability analysis performed earlier.

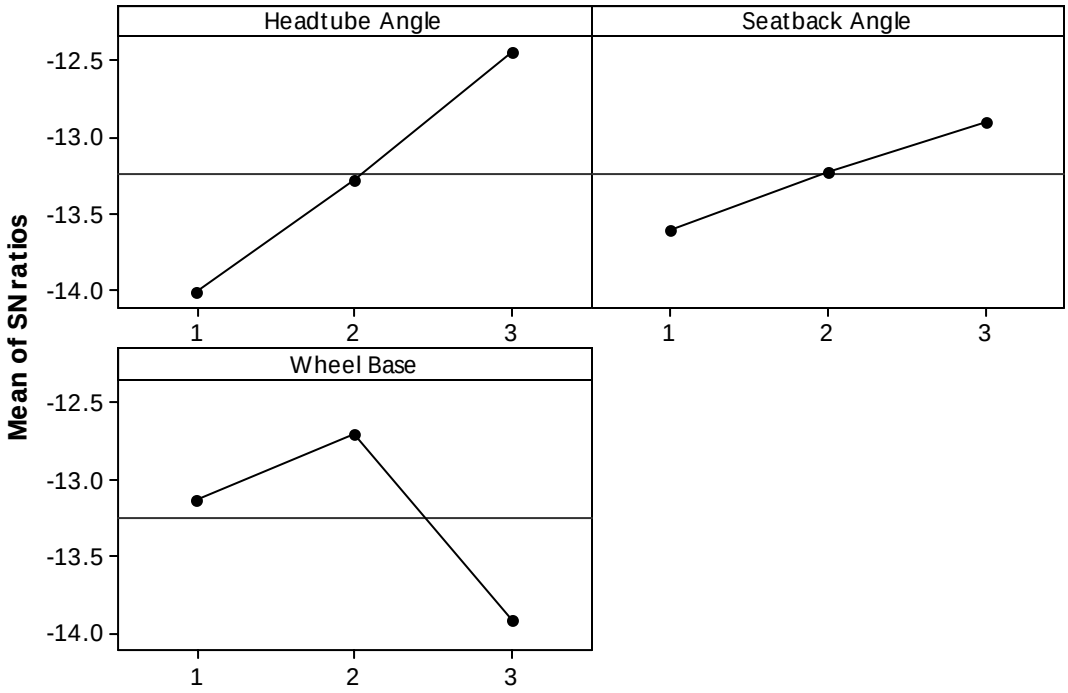

Figure 15 - Stability Results

Table 9 shows the results of analyzing the bicycle geometry using equation 2. It is evident that analysis and testing agree because the best configurations according to Taguchi have high K5 values. Furthermore, it can be seen that headtube angle which creates trail has the most important effect on stability since its signal to noise ratio is largest and it dominates the K5 stability analysis.

Table 9 - Stability Analysis Results

Configuration			K5
Headtube	Seatback	Wheelbase	
1	1	3	0.17
1	2	3	0.18
1	1	2	0.19
1	3	3	0.20
1	2	2	0.21
2	1	3	0.23
1	3	2	0.23
1	1	1	0.24
2	2	3	0.25

1	2	1	0.26
2	1	2	0.26
2	3	3	0.27
1	3	1	0.27
2	2	2	0.29
2	3	2	0.31
2	1	1	0.32
2	2	1	0.35
2	3	1	0.37
3	1	3	0.43
3	2	3	0.48
3	1	2	0.50
3	3	3	0.52
3	2	2	0.55
3	3	2	0.60
3	1	1	0.62
3	2	1	0.67
3	3	1	0.71

Finally, to confirm the results of Taguchi, the closest match of the best and worst control factor settings were compared with an overall average of all steering deflections in figure 16. Note that exact configurations could not be used because the Taguchi L_9 method only requires 1/3 of the total possible configurations. The graph shows that the best configuration according to Taguchi does indeed have a low deflection, while the worst configuration has a high deflection.

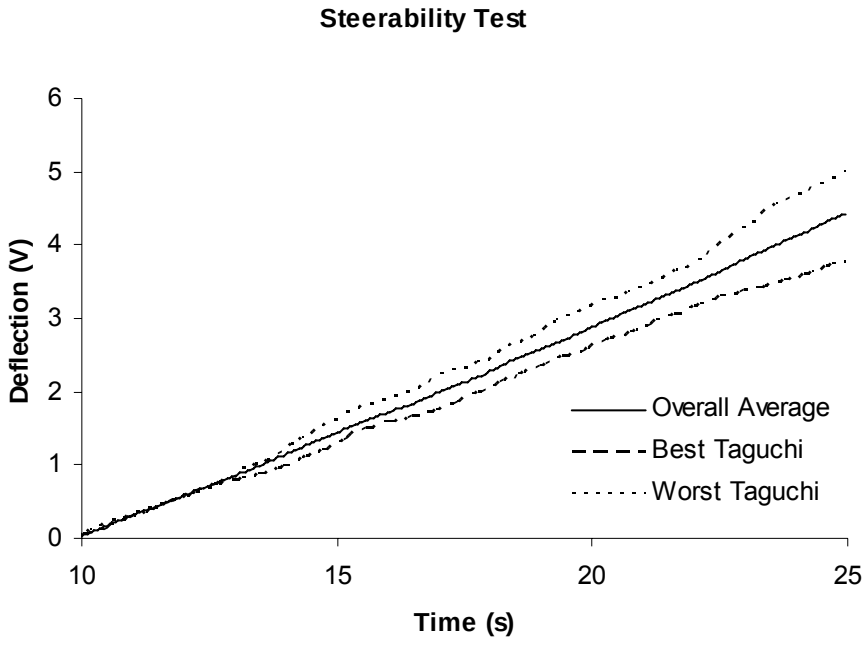

Figure 16 - Stability Deflection Averages

3.2 Abrasion Resistance

In order to ensure the safety of our riders, competitors, and bystanders, we performed skid testing. To accomplish this task, we prepared samples of various materials to a do skid testing. Each sample was weighed with .56 lbs per inch^2 of surface area. This is an estimate for the loading on one square inch of the bike if the vehicle were to slide on its side. The materials were then released onto an asphalt surface at a velocity of 30 mph. The distance that each sample slid was measured and recorded along with any observations about damaged sustained by the material. Each sample was put through three trials.

This testing served two purposes. Its first purpose was to determine how far our bike would skid if it were to crash so that we could predict whether a particular material would cause our bike to slide excessively. Our goal was to reduce the distance our bike would slide because we did not want to risk using a material which might cause our vehicle to slide into other vehicles or spectators. The material which slid the furthest was the Kevlar sample having a weave that was with the direction of the velocity. This material had an average skid distance of 80 feet. The material which slid the least distance was the Kevlar sample, having a weave that was at an angle of 45˚ with the direction of the velocity. This sample slid an average of 55 feet per trial. The second purpose of the skid testing was to ensure that the material would retain its structural integrity after crashing. Because Infinity has a monocoque design, the structural integrity of the bike relies heavily upon the durability of the fairing. Therefore, it is extremely important that the materials chosen to construct the bike can withstand the wear and tear caused by any crashes which might occur. According to our observations, the two materials which were least damaged in the testing process were the Kevlar material with the weave running along the direction of the velocity and the carbon-Kevlar hybrid material with the carbon weave laid perpendicular to the velocity and the Kevlar laid parallel to the velocity.

Based upon these results, we decided to use the carbon-Kevlar hybrid material with the carbon weave laid perpendicular to the velocity and the Kevlar lay parallel to the velocity. The surface of this material sustained the least amount of damage during testing and was the only material in which all strands were left intact. The material which came the closest to matching this material's durability was the Kevlar material with the weave running along the direction of the velocity. However, this Kevlar sample also had the largest sliding distance, so we chose the safer alternative.

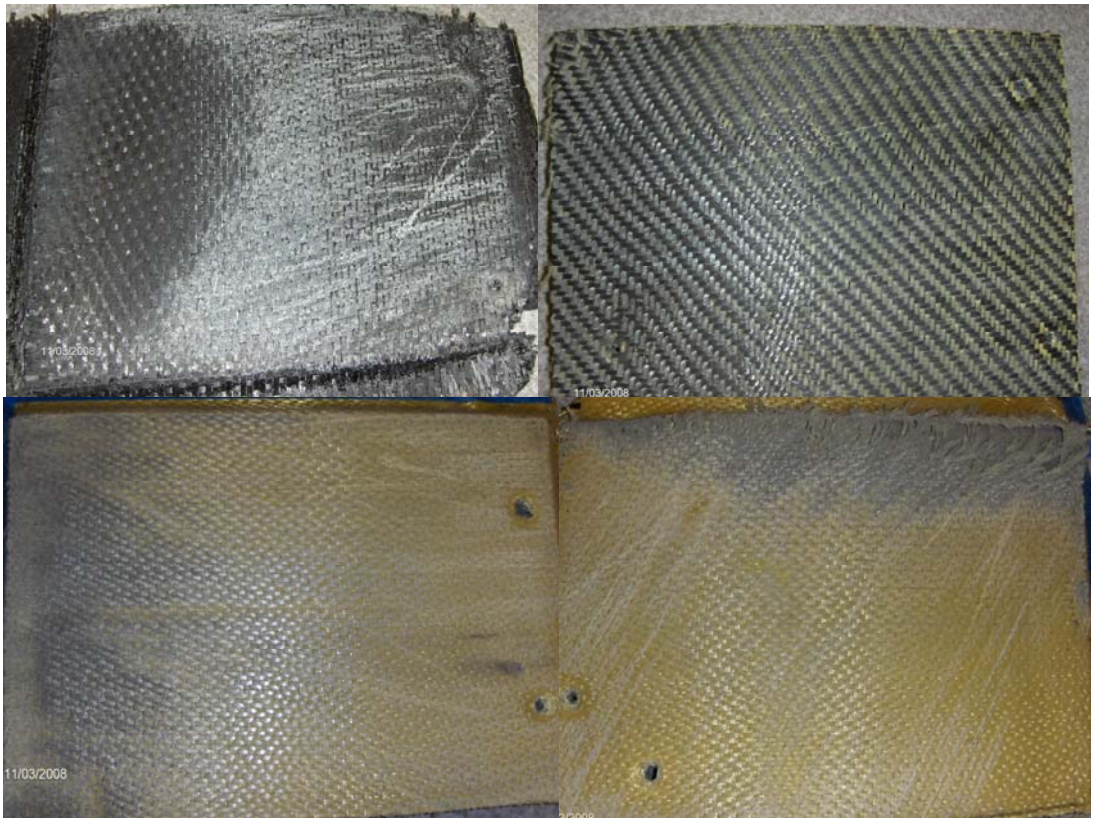

Figure 17 - (Top Left) Carbon fiber sliding test sample. Notice excessive wear and the loss of many fibers. (Top Right) Hybrid fabric shows great resistance to sliding. Notice that all fibers are left intact. (Bottom Left) Kevlar that slides well still seems to show wear and a few broken fibers. (Bottom Right) Another failure mode for Kevlar is to fuzz up: this destroys the fibers.

3.3 3 Point Bend Test

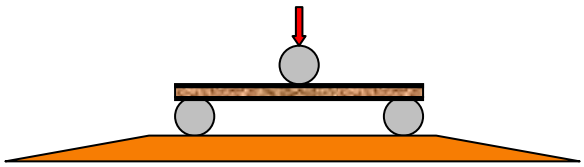

Figure 18 - 3 Point Bend Test Setup

A three point bending test was used to determine the material properties of test samples of various composite sandwiches. These samples were varied in core material, number of layers and type of fabric In the test, the maximum force applied over a given deflection was recorded in a tensile tester. It was observed that nearly all the samples failed in shear in the core material. There were a few samples whose failure mode was delamination of the carbon fiber from the core material, but those samples were not considered for use in

the final design. Since the samples failed in shear in the center, there is a formula which can be used to determine the shear stress at which the sample failed:

Equation 9

$$\tau_{Sample} = \frac{F \cdot T^2 b}{16\left(\frac{bT^3}{12} - \frac{b(T-0.21)^3}{12}\right)b}$$

Using this as the shear strength of the material, we then use Mohr's Circle to find that the principal shear stress equaled the principal bending stress. As a result, we are able to calculate the maximum amount of weight our bike will support. For this calculation, the bike was modeled as a hollow semicircle.

Equation 10

$$I_{Bike} = \int_0^{\pi}\int_9^{9.5}\left[(r^2\sin(\theta))^2(r \cdot dr \cdot d\theta)\right]$$

Equation 11

$$\tau_{Bike} = \tau_{Sample} = \sigma_{Bike} = \frac{W \cdot L_{Wheelbase} y}{4I_{Bike}}$$

Equation 12

$$W = \frac{4\sigma_{Bike} I_{Bike}}{L_{Wheelbase}\,\bar{y}}$$

The calculated weight that our bike could hold is about 1500 lbf which equates to a factor of safety of 7.5 given a rider and vehicle weight of 200 lbf. The following shows error analysis of these results.

Below is the overall equation for the weight, W. It is a function of applied force F, base width b, thickness T, length between the wheel supports L, and the two radii for the outer shell of the fairing and the inner shell of the fairing r_1 and r_2. I is the moment of inertia and is considered a constant for this uncertainty analysis.

Equation 13

$$W = \frac{4FT^2 I}{\frac{4}{3}bT^3 - \frac{4}{3}b(T-0.21)^3 L\left(\frac{2}{3}r_1^3 - \frac{2}{3}r_2^3\right)}$$

In order to find the uncertainty in the weight, the partial derivatives of F, T, and b were taken. These partials were squared to find the weighting factors of each of the sources of uncertainty in the measurements.

Equation 14

$$w_{weight}^2 = \frac{16T^4I^2}{\left(\frac{4}{3}bT^3 - \frac{4}{3}b(T-0.21)^3\right)^2 L^2\left(\frac{2}{3}r_1^3 - \frac{2}{3}r_2^3\right)^2} w_{Force}^2 + \left(\frac{8FTI}{\left(\frac{4}{3}bT^3 - \frac{4}{3}b(T-0.21)^3\right)L\left(\frac{2}{3}r_1^3 - \frac{2}{3}r_2^3\right)} - \frac{4FT^2I\left(4bT^2 - 4b(T-0.21)^2\right)}{\left(\frac{4}{3}bT^3 - \frac{4}{3}b(T-0.21)^3\right)^2 L\left(\frac{2}{3}r_1^3 - \frac{2}{3}r_2^3\right)} \right)^2 w_{Thicknes}^2 + \left(\frac{16F^2T^4I^2\left(\frac{4}{3}bT^3 - \frac{4}{3}b(T-0.21)^3\right)^2}{\left(\frac{4}{3}bT^3 - \frac{4}{3}b(T-0.21)^3\right)^4 L^2\left(\frac{2}{3}r_1^3 - \frac{2}{3}r_2^3\right)^2} \right) w_{base}^2$$

Equation 15

$$w_{weight}^2 = 0.32w_{Force}^2 + 83387.31w_{Thickness}^2 + 1284.38w_{base}^2$$

The nominal values were substituted into the equation to get the relationship above. It is clear that the measurement of T is the most sensitive in this form. The thickness and base widths were measured with a pair of digital calipers. Due to the accuracy of the calipers, the force measurement actually contributes 43.5% of the error overall.

Equation 16

$$w_{weight} = 4.5lb$$

Weight has a nominal value of 107.5 ± 4.5 lbf, the percent error of the measurement was 4.2.

3.4 Roll Cage Testing

A mock up of the roll cage that is in our bike was constructed using layers of (starting on the inside) 1 layer of Kevlar, 3 layers of carbon fiber, Nomex honeycomb core, 3 layers of carbon fiber, and a layer of Kevlar and carbon fiber bi-weave. The layers were vacuum-formed to the mold and allowed to dry. Once the roll cage was completed, it was placed in a tensile test machine in the vertical orientation. A load of 507 lbf was applied to the roll cage. Next the roll cage was loaded in the side load orientation. A load of greater than 269 lbf was applied. In both load cases, the roll cage demonstrated that it met the requirements for load carrying and for deformation, and exceeded the amount necessary to satify the rules and the error in the tensile tester. (+/- 8 lbf)

Figure 19 - Carbon fiber roll cage

After it was established that the roll cage met the specifications from the rule book, it was decided to reload the roll cage in the vertical orientation, and a force of 765 lbf was applied before there was significant deformation. The Nomex honeycomb demonstrated a remarkable resilience in that after it was deformed, it recovered to its original shape and material properties. Subsequent testing also showed the durability of the roll cage after various alternate loadings. To view videos of the Roll Cage testing please visit http://www.rose-hulman.edu/hpv/testing/2008/ASME/ .

4 Safety

The overall goal for the 2008 Infinity is to design a safer, more stable vehicle than the previous year. Thus, every effort has been made to take safety into account in the testing, analysis and design of the vehicle The monocoque shell provides the rider with unparalleled rollover and side protection, with an integrated roll cage into the fairing design. This ensures that no part of the rider could ever touch the ground while riding the vehicle, or in any failure mode. The rider will also be anchored to the vehicle via a four-point seat belt harness. Finally, the rider's visibility will be greatly improved over our previous vehicle, as a flat sheet will be bent to ensure maximum clarity. With all these safety features, the Rose-Hulman Infinity will be the safest HPV on the course.

Appendix 1 Abrasion Resistance Data

Material	Direction of Weave	Skid Distance (feet) Trial 1	Trial 2	Trial 3	Ave	Additional Observations
Carbon	Vertical	58	61	61	60	severe abrasion, worn through in some areas, complete loss of some fibers
Carbon/Kevlar Hybrid	Carbon-Lengthwise, Kevlar-Vertical	76	71	75	74	minor abrasion, all carbon strands intact, all Kevlar intact, minor Kevlar fuzzing
Carbon	Horizontal	67	74	72	71	moderate to severe abrasion on 20% of surface, nickel-sized patch of missing fibers
Kevlar	With weave	78	81	80	80	minor fuzz across entire surface, significant fuzz across 20% of surface, few fibers missing
Carbon/Kevlar Hybrid	Carbon-Vertical, Kevlar-Lengthwise	77	66	58	67	severe Kevlar fuzz over 5% of surface, missing carbon and Kevlar fibers, excessive fuzz on tail end
Kevlar	45˚ angle with weave	58	53	53	55	severe Kevlar fuzz, quarter-sized patch of missing fiber, minor fuzzing across 30% of surface, some delamination

Appendix 2 Costs

Table 10 - Parts List

Description	Qty	Unit Cost (USD)	Total (USD)	Purchased from
Cranks	1	59.50	59.50	QBP
Shimano Freehub Body (Deore M525)	1	11.70	11.70	QBP
Shimano Shifters (LX MTB flatbar)	1	55.20	55.20	QBP
Brakes (Hayes Disc)	2	52.65	105.30	QBP
Rims (AlexDX32)	1	28.00	28.00	QBP
Rims (AlexDA16)	1	13.75	13.75	QBP
Aluminum for Hubs	1	100.00	100.00	MetalsDepot.com
Custom spokes/Nipples	1	40.00	40.00	Local Shop
Tires (Ecorun)	1	65.00	65.00	REV Team
Tires (Stelvio)	1	24.96	24.96	QBP
Cassettes	1	49.00	49.00	QBP
Brake cable housing and ends	1	4.95	4.95	QBP
Gear cable housing and ends	1	4.95	4.95	QBP
Derailleur	1	54.24	54.24	QBP
Cranks/Bottom Bracket	1	100.00	100.00	Nashbar
Chain	2	7.68	15.36	QBP
4pt seat belt	1	30.00	30.00	Ebay
Tubes	2	1.51	3.02	QBP
Carbon from (purchased last year)	30	45.00	1,350.00	Hed
Carbon (purchased this year)	6	62.00	372.00	Hed
Carbon	15	41.50	622.50	U.S. Composites
Kevlar	13	22.00	286.00	U.S. Composites
Hybrid	6	34.50	207.00	U.S. Composites
Epoxy (gallons)	4	52.00	208.00	U.S. Composites
Nomex (40"X100" Sheet)	1	500.00	500.00	Fibreglast.com
Total				

Table 11 - Overall Expenditures

Employees (Qty)	Cost (USD)
Welder (1)	2,500
Machinists (3)	7,500
Workers (5)	13,867
Engineer (1)	3,750

Capital Costs	
Building Rent	3,000
Utilities	1,000
Equipment	1,000
Advertising	1,000
Shipping	750
Plug Construction	1,785
Cost per Month	36,152
Additional cost per unit	4,310.43
Total cost per unit	7,925.60

References

[1] Beauchamp, W., “Streamliner Scale Sizing Project,” Streamliner sizes information, http://www.recumbents.com/WISIL/scale_project/streamliners.htm

[2] Beauchamp, W., “The Varna Team” Information on WHPSC participants, http://www.recumbents.com/WISIL/whpsc2004/Varna.htm

[3] Beauchamp, W., “The Blue Yonder Team” Information on WHPSC participants, http://www.wisil.recumbents.com/wisil/whpsc2001/Blue_Yonder_Team.htm

[4] Ficarra, M. V., 2003, “iMike,” humanoid CAD model, http://www.xanadu.cz/download.asp?file=iMike

[5] Juvinall, R. C., and Marshek, K. M., 2006, “Fundamentals of Machine Component Design”, John Wiley & Sons Inc., pp. 147.

[6] Owers, D, J., 1985 “Development of a Human-Powered Racing Hydrofoil,” Human Power, 3, “3” pp. 13

[7] Patterson, W. B., 2004, *The Lords of the Chainring* Santa Maria